Optimizing Non-Contrast 3D Aortic Morphology MRI with Compressed Sensing

Emilie Bollache[1], Louisa Sefsaf[1], Mina Moeini[1], Shannon Soulez[1], Clément Patrizio[1], Daniel Giese[2], Alban Redheuil[1,3,4], Khaoula Bouazizi[1,3], Nadjia Kachenoura[1]

[1]Sorbonne Université, Inserm, CNRS, Laboratoire d'Imagerie Biomédicale, Paris, France
[2]Research & Clinical Translation, Magnetic Resonance, Siemens Healthineers AG, Erlangen, Germany
[3]Institute of Cardiometabolism and Nutrition (ICAN), Paris, France
[4]Sorbonne Université, AP-HP, Imagerie Cardiovasculaire et Thoracique, Institut de Cardiologie, Hôpital Pitié-Salpêtrière, Paris, France

Abstract

Accurate evaluation of aortic size is crucial in aortic disease. We aimed to compare non-contrast-enhanced MRI acquisition strategies, to define the optimal balance between scan time and reliable quantification of 3D aortic morphology. Forty-eight healthy volunteers (39±14 years, 29 women) underwent aortic MRI using the clinical reference sequence and 4 accelerated strategies using compressed sensing (CS) with either fat saturation (fs), spectral adiabatic inversion-recovery (SPAIR) or Dixon fat-water separation. Aortic diameter at 7 anatomical locations, length and volume of 4 aortic segments were measured from each dataset. CS strategies were significantly faster than the reference (1:38±0:32 to 3:12±0:55 vs. 7:42±2:27 min, all p<0.0001), and provided reliable measures as revealed by high correlation coefficients with the reference (r≥0.88) and low Bland-Altman biases, which also ranged within inter-operator variability (diameter≤0.57[-3.0;4.1]mm, length≤0.69[-14;15]mm, volume≤0.54[-8.9;9.9]ml). Diameters and volumes significantly increased from 20-35 to 50-70 years (p≤0.01) when considering fs and SPAIR strategies with area under ROC curves ranging from 73 to 91%, being the highest for fs. Non-contrast MRI sequence combining CS and fat saturation achieved reliable assessment of 3D aortic morphology while reducing scan time by 3.

1. Introduction

The thoracic aorta is exposed to atherosclerosis and degradation of elastic wall fibers related to continuous heartbeat-generated mechanical and hemodynamic stresses as well as age-related increase in arterial pressure. Such stresses and changes are further amplified in the presence of inflammation and risk factors such as hypertension, diabetes or obesity. Age- and disease-related aortic alterations are reflected by changes in aortic geometry, function and inner blood flow hemodynamics, which in turn increase the load exerted on the left ventricle. However, despite these multifaceted changes, to date, only inner arterial diameter measured from 2D imaging is considered for aortic disease prognosis, progression evaluation and hence patient risk stratification and subsequent decision-making regarding treatment or surgery.

Radiation-free Magnetic Resonance Imaging (MRI) through its excellent image quality, numerous "sequences" and extended anatomical coverage can uniquely provide non-invasive, comprehensive *in vivo* 3D evaluation of the thoracic aorta. Among MRI sequences used for vascular assessment, angiography provides information on arterial anatomy and geometry including presence of stenosis and atherosclerotic plaque [1]. Quantitative, comprehensive 3D morphological characterization includes aortic diameters, length and volume. As such, MRI is today recommended over computed tomography (CT) in selected patients with aortic disease to avoid excessive exposure to radiation including in repetitive follow-up, during pregnancy or in young patients [2]. Importantly, research studies in small series and various aortic conditions have been supporting the use of contrast-free over standard contrast-enhanced MRI angiography to evaluate aortic morphology [3-5].

However, to date there is no consensus as to the optimal MRI aortic angiographic strategy for comprehensive assessment of aortic morphology. This is partly due to multiplicity and customization of available MRI sequences, which mostly still require lengthy scan times. Indeed, MRI sequences can be tuned by the radiologic technologist during the exam through settings such as spatial resolution, which has a direct impact on both scan time and image quality: when resolution is finer, level of detail in the image improves but noise increases, and the patient has to lie down longer inside the scanner. Accordingly, MRI is always a matter of defining the best compromise between required image quality and patient comfort.

This work aimed to compare different magnetic resonance angiography (MRA) acquisition strategies providing 3D morphology of the thoracic aorta without contrast agent injection. Sequence evaluation targeted optimal balance between scan time and reliable quantification of aortic diameters, lengths and volumes in healthy individuals.

2. Methods

2.1. Study group and MRI acquisitions

We included 48 asymptomatic healthy volunteers (39±14 years, 29 women) stratified into two age groups: 20-35 and 50-70 years. The following inclusion criteria were applied: body mass index <30 kg/m², no contraindication to MRI, no pregnancy or breastfeeding, no personal history or known cardiac disease. Institutional Review Board (IRB) approval was obtained, and each participant provided signed, informed consent.

Each individual underwent contrast-free MRA (1.5 Tesla, MAGNETOM Sola, Siemens Healthineers, Forchheim, Germany) of the 3D aortic volume (field of view = 257-262 x 350 x 64-110 mm^3) in parasagittal view during diastole while using ECG gating and respiratory navigator. First, a conventional gradient-echo pulse sequence with spectral fat saturation (fs) and an acquired spatial resolution = 1.28x1.42x2 mm^3 was used as reference (REF). Then, 3 research sequences accelerated with compressed sensing (CS) with isotropic spatial resolution = 1.3 mm^3 were applied using different fat signal suppression methods: fs (CS_{fs}, acceleration factor R = 5), spectral adiabatic inversion-recovery (CS_{SPAIR}, R = 5), or Dixon fat-water separation (CS_{Dixon}, R = 7). Finally, a fourth research sequence was performed using CS, R = 5, fs and spatial resolution = 1.28x1.42x2 mm^3 similar to the reference ($CS_{resoREF}$).

2.2. Quantification of aortic morphology

Morphological indices were extracted from each MRA dataset, following semi-automated 3D aortic segmentation using a custom software (Mimosa, LIB, Sorbonne Université [6,7]). Thoracic aortic cross-sectional diameters were measured (Figure 1, purple marks) at the sino-tubular junction (STJ), mid-ascending aorta (AAo), proximal aortic arch at the level of brachiocephalic trunk (BCT), distal aortic arch at the level of left subclavian artery (LSA), proximal descending aorta (DAo) at the level of mid-AAo, distal DAo at the level of diaphragm and celiac trunk (CeTr). Lengths and volumes of AAo, aortic arch, proximal and distal DAo (Figure 1, orange arrows) were further derived according to European Society of Cardiology (ESC) guidelines.

Figure 1. Locations used to measure aortic diameters (purple) along with lengths and volumes (orange).

Of note, water-only images were considered for CS_{Dixon}. Image and segmentation quality was assessed visually, and measurement locations with failed aortic segmentation for at least one MRA sequence were excluded from further analyses. Throughout the whole image analysis process, operators were blinded to acquisition strategy and parameters.

2.3. Statistical analyses

Data were presented as mean ± standard deviation. Differences between each CS and reference MRA sequences, in terms of scan times and aortic morphological measures, as well as differences between the 2 age groups, were assessed using a Wilcoxon signed-rank test. Comparison of morphological measures between CS and reference sequences was further assessed using linear regressions and Bland-Altman analyses. Pearson correlation coefficients along with biases (= tested CS sequence – reference) and limits of agreement, as defined by mean bias ± 1.96 x standard deviation, were provided. Finally, the ability of each measure derived from each MRA sequence, to discriminate the previously reported effects of aging on aortic morphology by separating the 2 age groups, was assessed using a Receiver Operating Characteristic (ROC) curve. Areas under curve (AUC) were provided and paired comparison between AUC was achieved using DeLong test.

3. Results

3.1. Scan time and image quality

As expected, all CS MRA sequences were significantly faster (CS_{fs}: 2:56±0:51 min; CS_{SPAIR}: 3:03±0:59 min, CS_{Dixon}: 3:12±0:55 min, $CS_{resoREF}$: 1:38±0:32 min; all $p<0.0001$) than fs reference (7:42±2:27 min).

Representative examples of mid-thoracic aortic slice imaged using each reference, CS_{fs}, CS_{SPAIR}, CS_{Dixon} and $CS_{resoREF}$ MRA sequences are provided in Figure 2. Aortic segmentation and image quality were higher for reference (0 measurement exclusion) than for CS sequences, as diameter measurements / length and volume measurements were excluded in 3% / 4% cases for CS_{fs}, 5% / 6% for CS_{SPAIR}, 4% / 5% for CS_{Dixon} and $CS_{resoREF}$, respectively.

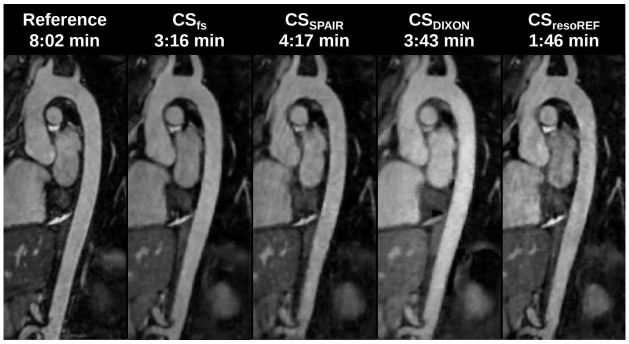

Figure 2. Examples of mid-thoracic aortic slice along with scan time obtained using each 3D aortic MRI angiography sequence in a 27-year-old healthy man.

3.2. Aortic morphological measures

Aortic diameters, lengths and volumes derived from each reference and tested CS MRA at the remaining measurement locations are provided in Figure 3. Although some statistical differences were observed between CS and reference sequences, overall agreement with the reference was confirmed when combining all measurement locations (Table 1), as revealed by high correlation coefficients (CS_{fs}: $r \geq 0.93$; CS_{SPAIR}: $r \geq 0.92$, CS_{Dixon}: $r \geq 0.88$, $CS_{resoREF}$: $r \geq 0.92$) and low Bland-Altman biases (diameter ≤ 0.57 [-3.0;4.1] mm, length ≤ 0.69 [-14;15] mm, volume ≤ 0.54 [-8.9;9.9] ml).

Table 1. Comparison of aortic morphology measures derived from each 3D CS MRA sequence against conventional reference, while combining all locations.

		CS_{fs}	CS_{SPAIR}	CS_{DIXON}	$CS_{resoREF}$
	Corr.	0.93, p<0.0001	0.92, p<0.0001	0.88, p<0.0001	0.92, p<0.0001
Diameter	Bias [LOA] (mm)	0.04 [-3.2;3.2]	0.08 [-3.2;3.4]	0.03 [-4.4;4.4]	0.57 [-3.0;4.1]
	Diff. (%)	6.2±6.6	6.4±6.9	8.8±8.4	7.1±7.1
	Corr.	0.97, p<0.0001	0.98, p<0.0001	0.97, p<0.0001	0.98, p<0.0001
Length	Bias [LOA] (mm)	0.37 [-18;19]	-0.01 [-17;17]	0.31 [-18;19]	0.69 [-14;15]
	Diff. (%)	9.4±8.4	9.0±8.3	9.7±8.5	8.5±7.6
	Corr.	0.94, p<0.0001	0.94, p<0.0001	0.91, p<0.0001	0.93, p<0.0001
Volume	Bias [LOA] (mL)	-0.31 [-8.9;8.3]	-0.50 [-9.2;8.2]	-0.21 [-11;10]	0.54 [-8.9;9.9]
	Diff. (%)	14±12	15±14	18±16	16±15

Corr.: Pearson correlation coefficient, LOA: Bland-Altman limits of agreement and Diff.: percentage absolute difference against reference, respectively.

3.3. Sensitivity to age-related variations

The 20–35 and 50–70-year-old subgroups included 29 (15 women, 28±3.6 years) and 19 (14 women, 56±4.0 years) volunteers, respectively. Morphological measures were significantly increased in older individuals, as compared to younger individuals ($p \leq 0.01$), except for aortic arch and distal DAo length derived from all sequences, as well as SJT diameter derived from CS_{Dixon} and $CS_{resoREF}$.

Finally, when considering measures that were significantly different between the 2 age groups, AUC obtained using CS strategies were within the same ranges (CS_{fs}: 73-91%; CS_{SPAIR}: 76-90%, CS_{Dixon}: 74-88%, $CS_{resoREF}$: 72-87%) as reference (73-90%). AUC was significantly lower for $CS_{resoREF}$ when compared to reference as well as other CS strategies for at least one measurement location. In addition, CS_{SPAIR} and CS_{fs} provided higher AUC than reference MRA for proximal DAo diameter (AUC = 0.84 vs. 0.77, p = 0.03) and volume (AUC = 0.90 vs. 0.83, p = 0.02), respectively. All other AUC were statistically comparable.

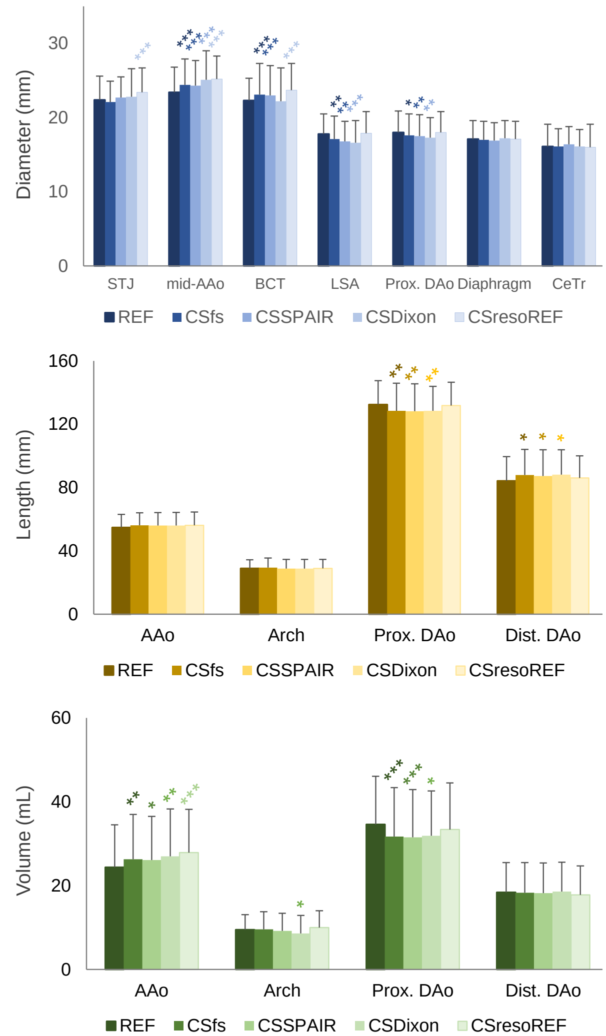

Figure 3. From top to bottom: diameter, length and volume mean values according to aortic anatomical location obtained using each 3D angiography sequence. *: p<0.05, **: p<0.01 and ***: p<0.001 against reference. Prox.: proximal, Dist.: distal.

4. Conclusion

Our main findings were: 1) all sequences accelerated with CS and factors R ranging from 5 to 7 were significantly faster than the clinical MRA reference sequence, 2) among tested CS sequences, MRA used with fat saturation (fs) and R=5 seemed to provide the overall best diagnostic image quality, 3) despite significant differences at some anatomical locations, all CS MRA provided good to excellent agreement with reference, 4) superior performances in discriminating the well-known physiological effects of ageing on aortic morphology, i.e. aortic dilation and elongation were observed when considering CS MRA based on fs or spectral adiabatic inversion-recovery (SPAIR) with R=5.

First, 3D aortic morphological measurements derived from MRA sequences were in agreement with previous literature [7]. Further consistency of CS-derived indices was demonstrated through comparison against the well-established clinical MRA reference, which resulted in high correlations and low biases. In addition, such biases ranged within intra-operator variability (diameter∼0.5 mm, length∼5 mm, volume∼2.7 ml [6]). Overall performances decreased when considering Dixon fat-water separation and R=7. In particular, both Dixon and $CS_{resoREF}$ (R=5) sequences seemed to provide lower ability to differentiate the 2 age groups. Of note, previous studies reported reliability of a Dixon-based CS MRA when compared to both fs-based conventional MRA and CT angiography references [8,9]; however, such studies were conducted at 3 Tesla and with a larger field of view in coronal orientation, allowing higher acceleration factor. Given the high sensitivity of fs and SPAIR methods to magnetic field heterogeneity, performance of such strategies at higher fields remains to be investigated.

In any case, future studies are required to establish MRA sequence-specific aortic disease severity thresholds before such techniques can be used in routine, as some significant differences and biases against current clinical reference were observed. Importantly, using the same sequence for longitudinal patient follow-up is of upmost relevance. Results we obtained in the current work should be taken with caution though due to the limited sample size. Observed differences between MRA datasets might also be due to confounding intra-operator variability in positioning anatomical landmarks. This should be addressed by image analysis pipelines integrating fully automated segmentation and identification of measurement location.

A 3D aortic MRA sequence combining compressed sensing accelerated by a factor of 5 and spectral fat saturation achieved high agreement and low biases with conventional reference sequence in terms of quantitative aortic diameters, lengths and volumes, within scan times that were on average 3 times faster, all without contrast. These findings remain to be confirmed on a larger sample size including participants with wider age and aortic geometry ranges and through independent validation. In the long term, our research aims to enhance patient comfort, improve aortic disease diagnosis and prognosis, and reduce MRI-associated waiting lists as well as costs.

Acknowledgments

We deeply acknowledge MRI technical staff (Awa Sidibé and Cécilia Ty) and project development manager Louise Meyfroit. Study was sponsored by Assistance Publique – Hôpitaux de Paris (Direction de la Recherche Clinique et de l'Innovation) and funded in part by internal Sorbonne University grant, ANR-10-IAHU-05 and ANR-24-CE19-3961-01.

References

[1] C. L. Dumoulin, and H. R. Hart Jr, “Magnetic resonance angiography,” *Radiology*, vol. 161, no. 3, pp. 717-720, Dec. 1986.

[2] E. M. Isselbacher et al., “ACC/AHA Guideline for the Diagnosis and Management of Aortic Disease: A Report of the American Heart Association/American College of Cardiology Joint Committee on Clinical Practice Guidelines,” *Circulation*, vol. 146, no. 24, pp. e334-e482, Dec. 2022.

[3] M. S. Krishnam et al., “Image quality and diagnostic accuracy of unenhanced SSFP MR angiography compared with conventional contrast-enhanced MR angiography for the assessment of thoracic aortic diseases,” *Eur. Radiol.*, vol. 20, no. 6, pp. 1311-1320, Dec. 2009.

[4] N. Kawel et al., “MR-imaging of the thoracic aorta: 3D-ECG- and respiratory-gated bSSFP imaging using the CLAWS algorithm versus contrast-enhanced 3D-MRA,” *Eur. J. Radiol.*, vol. 81, no. 2, pp. 239-243, Feb. 2012.

[5] S. Veldhoen et al., “Non-contrast MRA at 1.5T for aortic monitoring in Marfan patients after aortic root surgery”, *J. Cardiovasc. Magn. Reson.*, vol. 19, no. 1, pp. 82, Oct. 2017.

[6] T. Dietenbeck et al., “3D aortic morphology and stiffness in MRI using semi-automated cylindrical active surface provides optimized description of the vascular effects of aging and hypertension,” *Comput. Biol. Med.*, vol. 103, pp. 101-108, Dec. 2018.

[7] T. Dietenbeck et al., “Quantitative magnetic resonance imaging measures of three-dimensional aortic morphology in healthy aging and hypertension,” *J. Magn. Reson. Imaging*, vol. 53, no. 5, pp. 1471-1483, May 2021.

[8] M. G. Zeilinger et al., “Highly accelerated, Dixon-based non-contrast MR angiography versus high-pitch CT angiography,” *Radiol. Med.*, vol. 129, no. 2, pp. 268-279, Nov. 2023.

[9] J. Xing et al., “Improvement in Image Quality and Efficiency of Non-contrast Thoracic MR Angiography: Comparison of a Highly Accelerated Dixon-based Technique with the Conventional Fat-suppressed Technique,” *Magn. Reson. Med. Sci.*, vol. 25, no. 2, pp. 2025-0164, May 2026.

Address for correspondence:

Emilie Bollache
Laboratoire d’Imagerie Biomédicale – 15 rue de l’Ecole de Médecine – Escalier A, 3e étage – 75006 Paris, FRANCE
emilie.bollache@inserm.fr